Food Chemistry 452 (2024) 139532

Contents lists available at ScienceDirect

Food Chemistry

journal homepage: www.elsevier.com/locate/foodchem

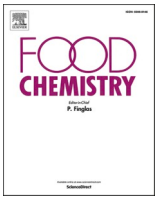

Absorption and intracellular accumulation of food-borne dicarbonyl precursors of advanced glycation end-product in a Caco-2 human cell transwell model

Xiyu Li [a,b,1,*], Wouter Bakker [a], Yaxin Sang [b,1,**], Ivonne M.C.M. Rietjens [a]

[a] Division of Toxicology, Wageningen University, PO Box 8000, 6700 EA Wageningen, the Netherlands
[b] College of Food Science and Technology, Hebei Agricultural University, Baoding 071000, China

ARTICLE INFO

Keywords:
Advanced glycation end products
Dicarbonyl compounds
Cytotoxicity
Caco-2 cell transwell model

ABSTRACT

This study aimed to better understand whether and how the reactive 1,2-dicarbonyl precursors of advanced glycation end products (AGEs), glyoxal (GO) and methylglyoxal (MGO), cross the intestinal barrier by studying their transport in the *in vitro* Caco-2 transwell system. The results reveal that GO, MGO and Nε-(carboxymethyl) lysine (CML), the latter studied for comparison, are transported across the intestinal cell layer *via* both active and passive transport and accumulate in the cells, albeit all to a limited extent. Besides, the transport of the dicarbonyl compounds was only partially affected by the presence of amino acids and protein, suggesting that scavenging by a food matrix will not fully prevent their intestinal absorption. Our study provides new insights into the absorption of the two major food-borne dicarbonyl AGE precursors and provides evidence of their potential systemic bioavailability but also of factors limiting their contribution to the overall exposome.

1. Introduction

Advanced glycation end-products (AGEs) result from non-enzymatic glycation reactions that occur widely in both the human body and during food processing. The formation of AGEs relies heavily on the presence of reactive 1,2-dicarbonyl compounds, with glyoxal (GO) and methylglyoxal (MGO) being among the most crucial and prevalent AGE precursors (Cha, Debnath, & Lee, 2019). AGEs and their precursors have been reported to cause a range of detrimental effects on human health (Yuan et al., 2021), including cell apoptosis, mitochondrial dysfunction, barrier dysfunction, inhibition of DNA repair enzymes and others (Cepas et al., 2021). Both processing and storage of food as well as endogenous physiological conditions can induce the production of AGEs and 1,2-dicarbonyl compounds, implying that both exogenous as well as endogenous sources may add to the total exposome (Hellwig, Gensberger-Reigl, Henle and Pischetsrieder, 2018; Rietjens et al., 2022). High levels of AGEs and 1,2-dicarbonyl compounds in blood plasma have been related to an increased risk of many diseases such as diabetes, uremia, and various types of cancer (Wang, Ma, Liu, Li and Gao, 2019). At present, there is a debate concerning whether the food-derived AGEs and 1,2-dicarbonyl compounds contribute to the endogenous pool and result in systemic physiological consequences after their intake (Delgado-Andrade and Fogliano, 2018; Delgado-Andrade, Tessier, Niquet-Leridon, Seiquer and Pilar Navarro, 2012; Förster, Kühne, & Henle, 2005; van Dongen et al., 2022).

A contribution of food-borne AGEs and their precursors to the total endogenous exposome clearly requires their systemic bioavailability upon oral intake. Thus, it is important to understand whether and how

Abbreviations: ACN, acetonitrile; AGEs, Advanced glycation end-products; ANOVA, Analysis of variance; ATCC, American Type Culture Collection; CE, Collision Energy; CML, Nε-(carboxymethyl)lysine; DMEM, Dulbecco's modified eagle medium; EDTA, Ethylenediaminetetraacetic acid; FBS, Fetal bovine serum; FL, Fructoselysine; GO, Glyoxal; HBSS, Hanks balanced salt solution; HEPES, 4-(2-hydroxyethyl)-1-piperazineethanesulfonic acid; HPLC, High-performance liquid chromatography; LAL, lysinoalanine; LC-MS, Liquid Chromatography–Mass Spectrometry; MGO, Methylglyoxal; NAM, New approach methodology; NEAA, Nonessential amino acids; P/S, Penicillin/Streptomycin; PBS, Phosphate buffered saline; 3Rs, Replace, Reduce and/or Refine; SPSS, Statistics for Social Science; TEER, Trans-epithelial resistance; Papp, Apparent permeability coefficient.

* Corresponding author at: Division of Toxicology, Wageningen University, Steepening 4, 6708 WE Wageningen, the Netherlands.
** Corresponding author.
E-mail addresses: xiyu.li@wur.nl (X. Li), yxsang1418@163.com (Y. Sang).
[1] Xiyu Li and Yaxin Sang both are contributed equally.

https://doi.org/10.1016/j.foodchem.2024.139532
Received 6 December 2023; Received in revised form 26 April 2024; Accepted 29 April 2024
Available online 30 April 2024

AGEs and 1,2-dicarbonyl compounds can cross the intestinal barrier. Some available literature data point at possible systemic bioavailability of food-borne AGEs and their precursors (Delgado-Andrade, Tessier, Niquet-Leridon, Seiquer and Pilar Navarro, 2012), while others argue against an important role of food-borne AGEs and their precursors due to their limited bioavailability, degradation, and/or scavenging by dietary components in the food or by the intestinal contents (Förster et al., 2005). Some reports have revealed that high molecular mass AGEs are not efficiently absorbed and need to be digested or degraded to low molecular mass AGEs before being absorbed (Hellwig, Matthes, Peto, Löbner and Henle, 2014). In contrast to the high molecular mass AGEs it appears that low molecular mass AGEs and their precursors have the potential to cross the intestinal barrier and enter the systemic circulation contributing to the endogenous exposure (van Dongen et al., 2022). Bioavailability upon oral intake has especially been reported for for example Nε-(carboxymethyl)lysine (CML) (Tessier et al., 2016), lysinoalanine (LAL), and fructoselysine (FL) (Somoza et al., 2006), while data on low molecular mass 1,2-dicarbonyl AGE precursors GO and MGO are limited. A study with healthy human volunteers reported that free MGO in the diet may not affect the excretion of MGO in the urine suggesting the contribution to the overall exposome to be limited (Degen, Vogel, Richter, Hellwig and Henle, 2013). However, whether the intestine can act as a barrier to completely limit the entry of GO and MGO into the body circulation still requires attention due to their strong reactivity and potential adverse effects. Moreover, intestinal cells may also provide a first site of contact and target for dietary AGEs and their precursors. Furthermore, the transport of AGEs *in vivo* can be influenced by a variety of factors, including the type of food matrix in which they are present and the presence of other substances in the intestinal lumen. In order to obtain more insight in the potential intestinal translocation and bioavailability of the dicarbonyl AGE precursors, further studies should be performed.

The Caco-2 cell transwell model is a well-established *in vitro* tool for assessing intestinal absorption, providing a new approach methodology (NAM) to replace, reduce and/or refine (3Rs) *in vivo* animal experiments (Bermudez-Brito et al., 2015). Caco-2 cells grown in layer on a transwell are known to exhibit many of the functional characteristics of intestinal cells after differentiation, including intestinal microvilli, intercellular tight junctions, and the apical well-defined brush border structure, and can secrete intestinal enzymes such as alkaline phosphatase (Awortwe, Fasinu and Rosenkranz, 2014). So far there have been a few studies reporting on the use of the Caco-2 cell model to study AGE absorption or AGE-induced injury in an *in vitro* model but none of these studies included the dicarbonyl AGE precursors. Wu et al. (2022) explored the transport and the effects of free and peptide-bound AGEs on energy homeostasis using the Caco-2 model system, and found that the free AGEs were the main regulator for cellular energy dysfunction. In another study, Wu et al. found that catechin can inhibit the absorption of protein-bound and free AGEs in the Caco-2 *in vitro* model by regulating the expression of tight intercellular junction proteins and PepT-1 (Wu et al., 2021). In line with this result, Wu et al. (2015) suppressed the oxidative stress and inflammation induced by dietary AGEs by the addition of lotus seedpod oligomeric procyanidins and catechin in the Caco-2 model system. Different AGEs have their own unique absorption characteristics and metabolic fate (Delgado-Andrade and Fogliano, 2018) with the problem being more complex for dicarbonyl AGE precursors due to their high reactivity. The potential for these precursors to chemically react with proteins and other amino structures or sulfur groups (Treibmann, Groß, Pätzold and Henle, 2022) has triggered the current scientific debate about their fate in the intestinal absorption process. Thus, the determination of intestinal absorption of the dicarbonyl AGE precursors is critical to better assess potential human health risks and the potential contribution of food-borne AGE precursors to the endogenous AGE levels and the total exposome.

Given their low molecular weight and intrinsic reactivity the low molecular mass AGE precursors MGO and GO are expected to be bioavailable, albeit only to a limited extent. Thus, the well-established Caco-2 cell model was used for investigating the transport of GO, MGO and, for comparison, of the low molecular mass AGE Nε-(carboxymethyl)lysine (CML), which has been shown to be bioavailable *in vivo* (Xu, Wang, Wang, Hu, & Liu, 2013). Transport was studied with and without protein to mimic the food matrix and potential scavenging of the reactive dicarbonyls preventing their transport, and at different temperatures (4 °C and 37 °C) to determine the passive or active nature of the transport. The findings will enhance our comprehension of the bioavailability and possible contribution of reactive dicarbonyl AGE precursors to the overall endogenous exposome.

2. Materials and methods

2.1. Chemicals and materials

GO (40% in water), MGO (40% in water), potassium dichromate and *o*-phenylenediamine were purchased from Sigma-Aldrich (St. Louis, MO, USA). CML was purchased from Biosynth Carbosynth (Bratislava, Slovakia). Dulbecco's modified eagle medium (DMEM) GlutaMAX, nonessential amino acids (NEAA), Penicillin/Streptomycin (P/S), trypsin, ethylenediaminetetraacetic acid (EDTA), 4-(2-hydroxyethyl)-1-piperazineethanesulfonic acid (HEPES), Hanks balanced salt solution (HBSS), and phosphate buffered saline (PBS) were obtained from Gibco (Paisley, UK). Cell Proliferation Reagent WST-1 was obtained from Roche (Mannheim, Germany). Fetal bovine serum (FBS) was provided by Bodinco (Alkmaar, The Netherlands). Transwell 24-well plates were from Corning Incorporated (Corning, New York, USA). For Liquid Chromatography–Mass Spectrometry (LC-MS), high-performance liquid chromatography (HPLC) grade solvents were used. All other reagents were of analytical reagent grade or purer.

2.2. Caco-2 cell culture

Human colon carcinoma Caco-2 cells were purchased from the American Type Culture Collection (ATCC) (Rockville, MD, USA). Caco-2 cells were cultured in DMEM GlutaMAX that contained 10% FBS, 1% P/S and 1% NEAA. The cells were incubated at 37 °C in a 5% CO_2 incubator.

The cell layer became confluent 3–5 days after seeding 1×10^6 cells/flask, and the cells were sub-cultured at a split ratio of 1:5 by trypsinization using 0.25% trypsin/10 mmol/L EDTA in PBS. The Caco-2 cells used in this study were within passages 10 to 40.

2.3. Cell cytotoxicity assay (WST-1 assay)

Cell cytotoxicity of CML and the dicarbonyl AGE precursors was analyzed using the WST-1 assay. To this end, Caco-2 cells were seeded at 3×10^4 cells / well in 96-well plates and cultured in a 5% CO_2 incubator at 37 °C for 20 days. The medium was refreshed every 2 days. Then, the medium was removed and replaced by 100 μL HBSS containing different concentrations of selected test compounds and cells were exposed for 2 h representing the same conditions and time interval as used for the transport experiments. After adding 5 μL Cell Proliferation Reagent WST-1 to each well, the plates were incubated at 37 °C for 1 h. Finally, absorbance was measured at 440 nm and 620 nm in a plate spectrophotometer (Molecular Devices, San Jose, CA, USA, Spectra Max M2). Samples with an absorbance value decrease of <10% compared to the control were considered viable and to reflect conditions suitable for transport studies.

2.4. Caco-2 cell model and integrity checking

When cells reached the subculturing density of 50–60% confluence (5.5×10^4 cells/cm^2), the medium in the flask was removed and cells were trypsinized using Trypsin-EDTA (Natoli, Leoni, D'Agnano, Zucco

and Felsani, 2012).[25] Cells were seeded at 3×10^4 cells/insert with 0.1 mL of the medium into the apical compartment of the 24-well transwell and 0.6 mL of complete medium was added to the basolateral compartment. The medium of both compartments was refreshed every two days.

The integrity of the cell membrane was assessed by transepithelial resistance (TEER) using Millicell ERS-2 (Billerica, MA, USA) after 14 days and then every 2 days. The Caco-2 cultures with a TEER value above 400 Ω/cm^2 were considered suitable for use in the transport experiment.

2.5. Transport of GO, MGO, and CML across Caco-2 cell layers

After 20 days, the medium in the inserts and wells was discarded and the cell layers were washed twice at 37 °C with the transport medium (HBSS containing 1% HEPES) and allowed to equilibrate with transport medium at 37 °C for 30 min. Then, 100 μL of transport medium containing different concentrations of the test compounds was added to the apical side and 600 μL of transport medium was added to the basolateral side and the transport time was recorded as 0 min. 60 μL of samples from the basolateral side were taken at time 0, 30, 60 and 120 min and replaced by fresh transport medium. Also 10 μL samples from the administered test solutions were taken at the start and 10 μL samples from the apical side were taken at the end of the 120 min incubation. The accurate administered concentration of every transport experiment were determined and used to calculate the apparent permeability coefficient (Papp) value for that experiment.

For transport experiments at different temperatures, transwell plates were placed at the same moment in a CO_2 incubator with different temperatures (4 °C and 37 °C). Other conditions were the same as those described above for the basic transport experiment.

For the studies simulating the presence of a food matrix, the transport experiments were performed in DMEM GlutaMAX (containing 1% P/S) with or without 10% FBS. In these experiments, 100 μL of corresponding medium containing different concentrations of the test compounds was added to the apical side. Other conditions were the same as those describe above for the basic transport experiment.

The Papp value of the three compounds (GO, MGO, CML) was calculated from the slope of the basolateral appearance of the compound according to the previously described equation:

$$P_{app}(cm/sec) = \frac{F \times V_D}{SA \times M_D}$$

where F is the flux rate (μmol/s), SA is the surface area for transport (0.33cm^2), V_D is the donor volume (mL), and M_D is the donor amount at $t = 0$ (μmol). All data represent the mean of triplicate experiments (Yee, 1997). The flux rate represents the amount of target compounds that can pass through the Caco-2 cell layer per unit time. The donor compartment refers to the apical side of the transwell in this study.

The flux rate represents the amount of target compounds that can pass through the Caco-2 cell layer per unit time. The donor compartment refers to the apical side of the transwell.

After taking the sample at the last time point included in the transport study, the medium from the apical side and basolateral side was aspirated and prewarmed HBSS was added to both sides. The TEER value was measured and compared with the starting value.

2.6. Intracellular accumulation of GO, MGO, and CML in the Caco-2 cells

After the transport experiment and measurement of the TEER value, the Caco-2 cell layer was washed with PBS at least 3 times carefully. The filter membrane was then cut out and added to an Eppendorf tube containing 200 μL 65% methanol. The Eppendorf tubes were kept on ice until and during sonification for 30 min. After that, the samples were centrifuged at 16000 ×*g* for 15 min at 4 °C and the supernatants were used for further analysis.

2.7. LC-MS/MS analysis of GO, MGO, CML and MGO-derived AGEs (CEL and MG-H1)

GO and MGO in the samples were derivatized basically as described by Zhou, Cheng, Gong, Li, and Wang (2019) and the resulting derivatives were subsequently measured by LC-MS/MS. In brief, 40 μL sample was mixed with 10 μL 50 mmol/L *o*-phenylenediamine in an Eppendorf tube. After mixing, the tubes were placed at 20 °C in the ThermoMixer F1 (Eppendorf Thermomixer Comfort, Germany) for 30 min and were ready for LC-MS/MS analysis that was performed immediately after the derivatization step. To quantify GO and MGO, standard curves were defined by derivatizing known concentrations of commercially available standards by the same procedure as described above.

A Shimadzu Nexera LC-40D XR UPLC system coupled to a Shimadzu LCMS-8045 triple quadruple mass spectrometer (Kyoto, Japan) was used for the analysis of the derivatized GO and MGO. 1 μL of the sample obtained after derivatization was injected into a Phenomenex Kinetex C18 column (50 × 2.1 mm, 1.7 μm) at 40 °C. The mobile phase consisted of a gradient of MilliQ water (MilliPore, USA) (including 0.1% (*v*/v) formic acid) and acetonitrile (ACN) (including 0.1% (*v*/v) formic acid) at a flow rate of 0.40 mL/min. The gradient started at 1% ACN, reached 25% ACN at 4 min, followed by 50% ACN at 6 min, then remained at 50% ACN until 7 min, returned to 1% ACN at 7.1 min, and remained at these initial conditions until 13 min. Under these conditions, derivatized GO eluted at 5.00 min, and derivatized MGO at 5.75 min. The LC-MS-8045 was equipped with an ESI source for MRM quantification in the positive ion mode. The following MRM transitions for each compound from precursor to product were selected for quantification: GO *m/z* 131.1 → 77.1 (CE = −35.0 V), MGO m/z 145.1 → 77.1 (Collision Energy (CE) = −35.0 V).

For analysis of CML, CEL and MG-H1, samples were measured by LC-MS/MS. 1 μL of the sample was injected into a UPLC Amide column (100 × 2.1 mm, 1.7 μm) at 40 °C without derivatization. The mobile phase consisted of a gradient of MilliQ water (including 0.1% (*v*/v) formic acid) and acetonitrile (including 0.1% (v/v) formic acid) at a flow rate of 0.30 mL/min. The gradient started at 75% ACN, reached 12.5% ACN at 5 min, and was kept at 12.5% until 11 min. Then, the gradient increased to 95% ACN at 12 min, was kept for 5 min at this condition, and then dropped to 75% ACN at 18 min, which was kept until 24 min. The flow started at 0.30 mL/min, and remained at this rate for 5 min, and was then followed by 0.15 mL/min until 13 min, and after that gradually increased to 0.20 mL/min, remaining at this rate until 15 min, and then returned to 0.30 mL/min, which remained until the end. Under these conditions, CML eluted at 4.65 min. The LC-MS-8040 was equipped with an ESI source for MRM quantification in the positive ion mode. The following MRM transitions for the compound from precursor to product were selected for quantification: CML *m/z* 204.9 → 84.1 (CE = −21.0 V), CEL m/z 219.05 → 84.25 (CE = −20.0 V) and MG-H1 m/z 229.15 → 70.20 (CE = −25.0 V). These compounds were quantified based on a calibration curve made with a commercially available standard. It should be noted that the standard curve of MG-H1 for quantification was a linear curve in HBSS and a quadratic curve in DMEM with or without serum, which is due to the reaction of MG-H1 with DMEM components.

2.8. Stability of GO and MGO in different media

To test the stability of GO and MGO in the different incubation or test media, GO and MGO were diluted in HBSS (containing 1% HEPES), DMEM without serum and DMEM with serum to 10 μmol/L, respectively. GO and MGO solutions in these different media were added to 24-well plates, incubated at 37 °C and sampled every 15 min from 0 min until 120 min. The percentage of the measured value from the starting

value ($t = 0$) at each time point was used to calculate the residual percentage of the test compounds as followed formula.

$$Residual\ percentage_t = \frac{\text{Concentration}_t}{\text{Concentration}_{initial}} \times 100\%$$

where the Concentration $_t$ is the concentration at the defined time point, Concentration $_{initial}$ is the initial concentration.

Subsequently, the concentration of MGO-derived AGEs (CEL and MG-H1) was measured on the poorly stabilized MGO reacting in different media for 0 min and 120 min.

2.9. Statistical analysis

For comparison, all results were expressed as mean values ± standard error of the mean (SEM). Statistical analyses were preformed using Statistics for Social Science (SPSS) version 28.0.1. For cytotoxicity experiments and transport experiments with different concentration of the compounds, one-way analysis of variance (ANOVA) was used to assess the significance of changes between different exposure concentrations followed by *post hoc* tests. For the assessment of differences between the different treatment groups, Student's *t*-test was used.

3. Results

3.1. Cytotoxicity of GO, MGO, and CML

Fig. 1 shows the effect of increasing concentrations of GO, MGO and CML on the viability of the Caco-2 cells. Based on these results concentrations of ≤ 750 μmol/L, ≤ 1000 μmol/L and ≤ 2000 μmol/L were considered adequate for the transport studies for GO, MGO and CML respectively.

3.2. Transport of GO, MGO, and CML across a Caco-2 cell layer

Fig. 2 presents the time dependent transport of GO, MGO an CML across the Caco-2 cell layer in HBSS at different concentrations. The concentration of GO, MGO and CML on the basolateral side increased with increasing exposure time and with increasing initial concentration at the apical side. The Papp values of GO, MGO and CML in the Apical (AP) to Basolateral(BL) direction derived from the linear part of these time-dependent curves are presented in Table 1. According to the Papp based absorption standard proposed by Yee (1997), a compound with a Papp value $<1 \times 10^{-6}$ cm/s is considered to be classified as a poorly absorbed compound whereas a compound with a Papp value between 1×10^{-6} cm/s and 1×10^{-5} cm/s is considered to be classified as moderately absorbed. Based on these criteria, CML is to be considered as being poorly absorbed, while GO and MGO are to be considered as being moderately absorbed. The transport decreased in the order: GO > MGO > CML.

Table 1 presents the distribution of GO, MGO, and CML over the apical, cellular and basolateral compartment at the end of the 120 min transport experiment. From these results it follows that for GO and MGO, the relative amount accumulated in the cells is low at all the test concentrations, whereas for CML at the same exposure concentration (125 μmol/L), the intracellular accumulation is 6.4- and 7.3- fold higher compared to that of GO and MGO. The results also show that the intracellular accumulation CML in the Caco-2 cells gradually increases with increasing concentrations, whereas the intracellular amount of MGO and GO does not show this increasing trend with increasing concentration. When expressed as percentage of the amount added at the apical part the relative intracellular accumulation appears to decrease with increasing concentration likely due to saturation of the underlying uptake. Intracellular accumulation percentage appeared most pronounced for CML, for which the accumulation upon 2 h incubation reached 4.5% of the total amount of CML added at an exposure concentration of 125 μmol/L.

The percentage transport and the recovery is shown in Table 1 as well. For CML, the percentage of the initial amount transported over the Caco-2 cell layer during the 2 h incubation is the lowest, at <1%, while that for GO and MGO, in line with the Papp values, is almost twice and three times as high, although the overall values are still low. Of particular note is that the percentage recovery for all three compounds was much <100%, especially in the case of MGO, probably due to the poor stability of the compounds, their reaction with cell components and/or their conversion inside the cells.

3.3. Transport modes of GO and MGO

In addition, specific transport studies were performed to elucidate the role of passive transport and active transport in the mode of action by which the dicarbonyl compounds cross the intestinal cells. To this end the transport of GO or MGO 125 μmol/L at 4 °C and 37 °C was compared (Fig. 3). The results obtained indicate that for MGO, the transport at 4 °C is somewhat lower than that at 37 °C albeit not significant which suggests passive transport to play a major role. For GO, the transport is significantly higher at 37 °C than at 4 °C. The percentage of transport at 4 °C after 2 h is about half of that at 37 °C, demonstrating the presence of active transport, and also a contribution of passive transport.

Table 2 presents the percentage of transport, intracellular accumulation and recovery of GO and MGO at the end of the 120 min transport experiment at different temperatures. From these data, it can be seen that the recovery for GO and MGO in the transport experiment differed between the temperatures, especially for MGO, for which recovery is substantially lower at 37 °C than at 4 °C. This may be due to a the lower rate of chemical reactions of the dicarbonyls with cell components and the degradation of the dicarbonyl AGE precursors by the cellular

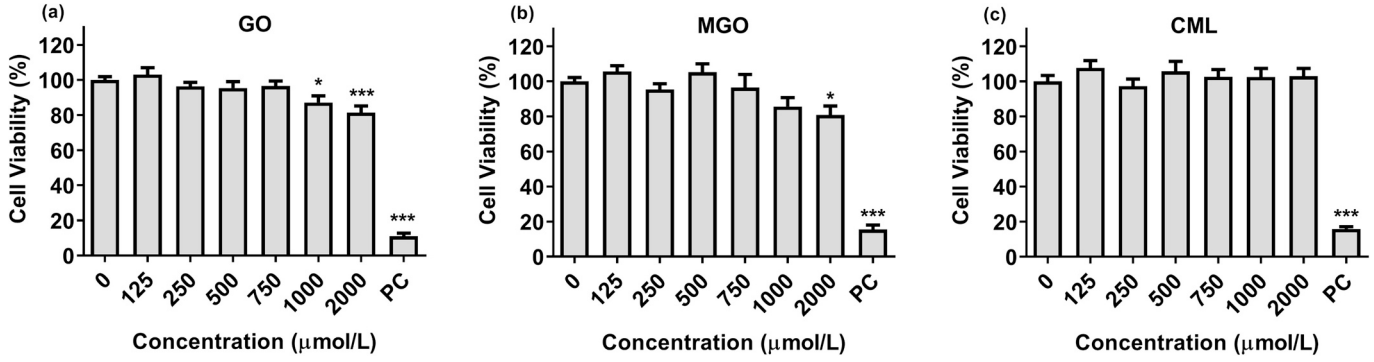

Fig. 1. Effects of a) GO, b) MGO, and c) CML on the viability of Caco-2 cells as determined by the WST-1 assay.
Notes: PC (Positive control): 15 mg/L K_2CrO_7 in HBSS * Represents $p \leq 0.05$, *** represents $p \leq 0.001$ based on comparisons made with group where the exposure concentration was 0 μmol/L. Data represent the mean of 3 independent measurements ± SEM.

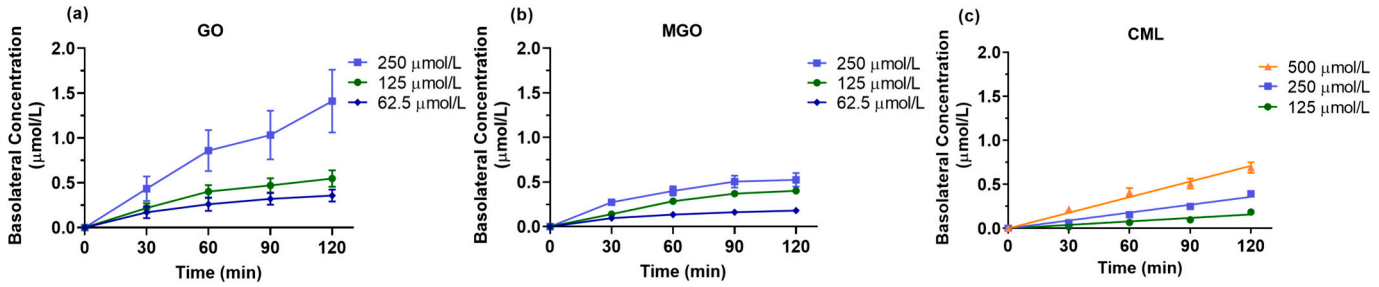

Fig. 2. Time dependent transport of a) GO, b) MGO, and c) CML across a Caco-2 cell layer at different concentrations in HBSS.
Note: Data represent the mean of 3 independent measurements ± SEM. To facilitate comparison all data were plotted using the same X and Y-axis.

Table 1
Percentage of the amount added at the apical side transported or accumulated in the cells and total recovery at the end of the Caco-2 cell layer transport studies with GO, MGO, and CML in HBSS.

Treatment	Concentration (µmol/L)	Papp value (cm/s) *	Intracellular accumulation amount (nmol)	Percentage (%) of the amount added at the apical side at t = 0			
				Apical side	Basolateral side	Intracellular accumulation	Recovery
GO	62.5	1.85×10^{-6} ^{a}	0.09 ± 0.11 ^{a}	71.0 ± 4.2 ^{a}	3.0 ± 1.6 ^{a}	1.3 ± 1.6^{a}	75.4 ± 5.2 ^{a}
	125	1.48×10^{-6} ^{a}	0.09 ± 0.11 ^{a}	80.1 ± 12.4^{b}	2.4 ± 1.7 ^{a}	0.7 ± 0.8^{ab}	83.2 ± 12.3 ^{a}
	250**	1.52×10^{-6} ^{a}	0.10 ± 0.10 ^{a}	74.7 ± 11.8^{ab}	3.3 ± 2.6 ^{a}	0.4 ± 0.4^{b}	78.4 ± 10.7 ^{a}
MGO	62.5	1.12×10^{-6} ^{ab}	0.17 ± 0.19 ^{a}	16.4 ± 8.3	1.8 ± 0.7 ^{ab}	2.8 ± 3.4 ^{a}	21.0 ± 11.2 ^{a}
	125	1.26×10^{-6} ^{a}	0.08 ± 0.13 ^{a}	24.2 ± 10.6	2.1 ± 1.0 ^{a}	0.9 ± 1.8 ^{b}	27.3 ± 10.6 ^{a}
	250	0.89×10^{-6} ^{b}	0.11 ± 0.15 ^{a}	18.7 ± 10.8	1.4 ± 0.7 ^{b}	0.5 ± 0.7 ^{b}	20.6 ± 11.1 ^{a}
CML	125	0.38×10^{-6} ^{a}	0.58 ± 0.22 ^{a}	80.9 ± 10.1 ^{a}	0.9 ± 0.2 ^{a}	4.5 ± 1.6^{a}	86.3 ± 9.7 ^{a}
	250	0.39×10^{-6} ^{a}	0.86 ± 0.45 ^{ab}	85.7 ± 6.7 ^{a}	0.9 ± 0.2 ^{a}	3.4 ± 1.9^{ab}	90.3 ± 7.7 ^{a}
	500	0.33×10^{-6} ^{a}	1.18 ± 0.70 ^{b}	82.4 ± 6.6 ^{a}	0.8 ± 0.2 ^{a}	2.2 ± 1.4^{b}	85.4 ± 7.3 ^{a}

Notes: * The Papp value is calculated here for GO and MGO from the first 60 min of transport data, whereas for CML, the data from the first 120 min are used. These time points represent the period during which transport appeared to be linear in time.
Means with different lowercase letters show a significant difference ($p \leq 0.05$) among different concentration groups of the compound.
** The Papp value at this concentration may be affected by a somewhat lower cell layer integrity as indicated by the somewhat lower TEER value at the end (67.8% of the initial value).

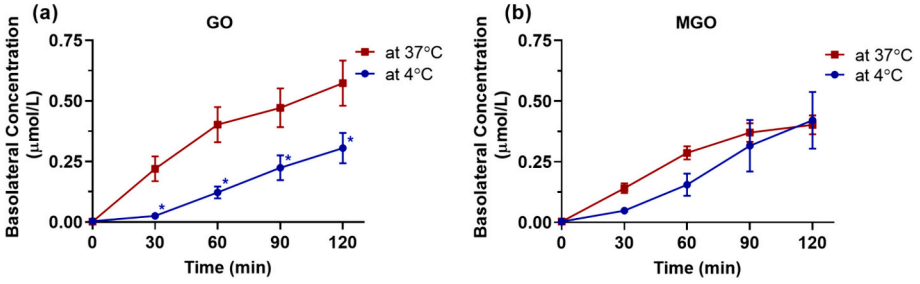

Fig. 3. Transport of (a) GO and (b) MGO at different temperatures (4 °C and 37 °C) in HBSS.
Note: The exposure concentration of Fig. 3 a) and b) is 125 µmol/L. Data represent the mean of 3 independent measurements ± SEM.
* indicates statistically different at 4 °C compared to 37 °C ($p \leq 0.05$).

Table 2
Percentage of the amount added at the apical side transported or accumulated in the cells and total recovery at the end of the 2 h Caco-2 cell layer transport studies with GO and MGO at 4 °C and 37 °C in HBSS medium at an exposure concentration of 125 µmol/L.

Treatment	Temperature (°C)	Papp value (cm/s)	Percentage (%) of the amount added at the apical side at t = 0			
			Apical side	Basolateral side	Intracellular accumulation	Recovery
GO	4	0.60×10^{-6} ^{a}	94.0 ± 11.3 ^{a}	1.4 ± 1.0 ^{a}	0.6 ± 1.0 ^{a}	96.3 ± 12.7 ^{a}
	37	1.48×10^{-6} ^{b}	80.1 ± 12.4 ^{b}	2.4 ± 1.7 ^{a}	0.7 ± 0.8 ^{a}	83.2 ± 12.3 ^{a}
MGO	4	0.68×10^{-6} ^{a}	82.7 ± 13.7 ^{a}	2.2 ± 1.9 ^{a}	0.2 ± 0.2 ^{a}	85.1 ± 13.4 ^{a}
	37	1.26×10^{-6} ^{a}	24.2 ± 10.6 ^{a}	2.1 ± 1.0 ^{a}	0.9 ± 1.8 ^{a}	27.3 ± 10.6 ^{b}

Notes: Means with different lowercase letters show a significant difference ($p \leq 0.05$) between different treatment groups.

detoxification system and metabolism at 4 °C. Further experiments were conducted to better understand how this reactivity of MGO affects its transport in the intestinal cell layer and the resulting bioavailability.

3.4. Effect of matrix constituents on transport of GO and MGO

To study the effect of food-derived matrix constituents that may enter the intestinal lumen together with GO and MGO on the intestinal transport and bioavailability of the dicarbonyl compounds, the transport of GO and MGO was studied using DMEM with or without added serum and results were compared to transport in HBSS. The results obtained are presented in Fig. 4 and reveal that the presence of amino acids in DMEM and of proteins and antioxidant enzymes in serum affected but not completely scavenged the levels and transport of GO and MGO. **Table S1** presents the Papp values and percentage recovery derived from the transport curves presented in Fig. 4. The presence of DMEM and serum and the resulting scavenging caused especially for MGO a rapid decline in the transport rate after the initial phase by >40% compared to the transport in HBSS (Fig. 4b). The recovery of GO and MGO without cells in these three media is presented in **Fig. 4(c)** and **(d)**. The results obtained reveal that GO and MGO underwent a greater degree of degradation and loss in DMEM, especially in the presence of serum (only 62.9% of GO and 42.7% of MGO remaining after 2 h of incubation), while in HBSS no decrease in their levels was observed. These results imply that the reduced recovery of GO and MGO in the transport experiment in HBSS (**Table S1**) may be due to their reaction with cells and also that the reduction in transport rate with increasing incubation time (Fig. 4(a) and (b)) can be ascribed to the reduced amount of GO and MGO available for transport following their scavenging by medium or cellular components. The differences in the results obtained in HBSS and DMEM (with or without serum) (Fig. 4) can be attributed to the reaction between the AGE precursors and components present in DMEM (with or without serum) and absent in HBSS such as arginine hydrochloride (84 mg/L in DMEM) and lysine hydrochloride (146 mg/L in DMEM). The data shown in **Table S1** reveal that scavenging by cellular components, amino acids and other medium and serum constituents is more substantial for MGO than for GO resulting in lower Papp values for MGO than GO in DMEM with serum.

Because of the poor stability of MGO in DMEM (with or without serum), in additional experiments the possible formation of MGO-derived AGEs (CEL and MG-H1) was quantified upon incubation of MGO in different media used in the present study, including HBSS and DMEM without and with serum. The results obtained are presented in **Fig. S1** (Supplementary materials) and show that in all media formation of CEL was below the limit of quantitation even upon 120 min incubation. Formation of MG-H1 was readily detected upon 120 min incubation in DMEM with the presence or absence of serum not affecting its formation to a significant extent, while MG-H1 formation was not observed in HBSS. Thus, amino acids present in the DMEM appear to be scavenging MGO resulting in AGE formation and reducing the amount of MGO available for cellular uptake and translocation.

4. Discussion

In recent years, concerns have been raised related to the hazards of foods containing AGEs (advanced glycation end-products) and their precursors (Ravichandran et al., 2019). To better understand the bioavailability of the dicarbonyl AGE precursors GO, and MGO in the human body, we conducted a study using the Caco-2 transwell model to simulate the intestinal barrier and compared the transport of GO and MGO to that of CML which is known to be bioavailable to a limited extent (Yuan et al., 2022; Yuan et al., 2023). Our findings suggest that GO and MGO can cross the intestinal cell layer, at a level that is limited (with 3.0% and 1.8% of the initial amount present at the apical side after 2 h incubation, respectively) (Table 1 **and** Fig. 2). However, this level is somewhat higher than that of CML for which <1% was transported within 2 h under similar transport conditions. Papp values were comparable at the different concentrations tested indicating that transport tended to be linear with the tested concentrations resulting in Papp values amounting to 1.48×10^{-6} cm/s for GO (125 μmol/L), 1.26×10^{-6} cm/s for MGO (125 μmol/L), and 0.39×10^{-6} cm/s for CML (125 μmol/L) (Table 1).

Several studies have reported on the possible modes of action for intestinal transport of a range of AGEs, but not precursors. Free low molecular mass (LMM) AGEs, for example, have been reported to enter the cells by simple diffusion rather than with transporters (Grunwald,

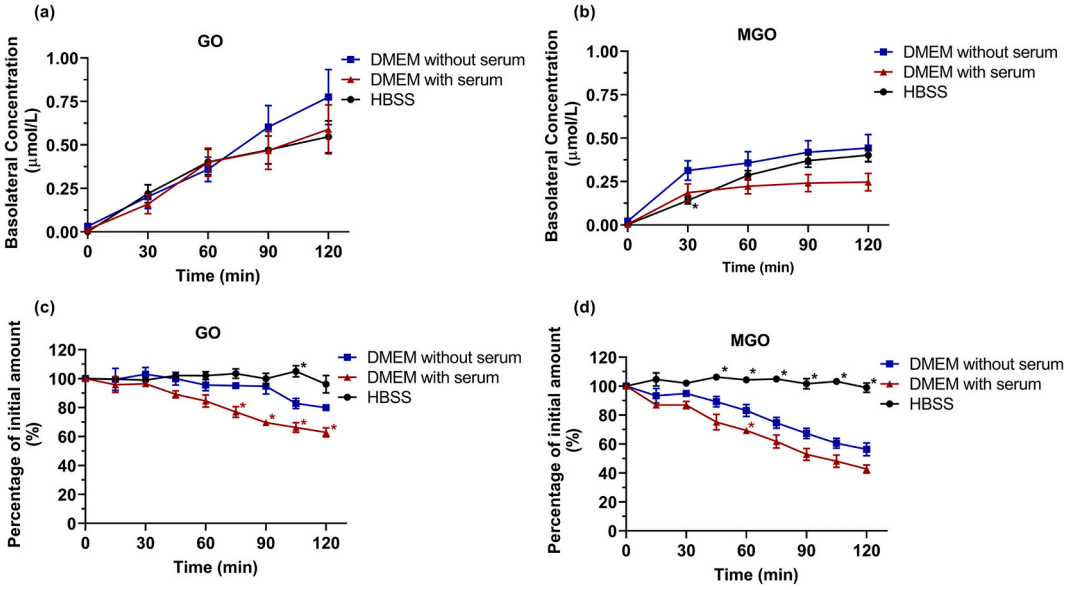

Fig. 4. Effect of matrix constituents on transport of a) GO and b) MGO across the Caco-2 cell layer and stability of c) GO and d) MGO in different media without Caco-2 cells.

Note: The exposure concentration of Fig. 4 a) and b) is 125 μmol/L.

* indicates statistically different in samples in HBSS (in black) or DMEM with serum (in red) compared to DMEM without serum ($p \leq 0.05$). (For interpretation of the references to colour in this figure legend, the reader is referred to the web version of this article.)

Krause, Bruch, Henle and Brandsch, 2006). Dipeptide-bound AGEs may be absorbed into the intestinal cells *via* the peptide transport protein PEPT1 (Hellwig et al., 2009; Hellwig et al., 2011). Some dipeptide-bound AGEs have been proven to be hydrolyzed intracellularly and subsequently undergo basolateral efflux (Hellwig et al., 2011). High molecular mass (HMM) AGEs may not be absorbed directly by the body. The difference in absorption and bioavailability between LMM and HMM forms of the same AGE or precursor can be attributed to the need for enzymatic degradation of HMM AGEs in the intestinal tract before absorption in an LMM form (van Dongen et al., 2022). Considering the hydrophilic nature of GO and MGO and the difficulty of crossing epithelial lipid membrane for these compounds, the non-energy-consuming transport part involved in this paper may be the passive paracellular route (Ding et al., 2021). Thus, the results for transport of dicarbonyl AGE precursors, as obtained in the present study, indicate that transport of MGO across the intestinal cell layer is mainly *via* this passive transport (Fig. 3). In contrast, GO appeared to employ a combination of passive and active transport mechanisms. Meanwhile, it is worth pointing out that the recovery of MGO at 37 °C was lower than at 4 °C (Table 2), probably due to the stagnant and slower reactions in cells, resulting in less efficient scavenging by for example enzymes such as *Glo1* and *Glo2* from the intact glyoxalase system (Wetzels, Wouters, Schalkwijk, Vanmierlo, & Hendriks, 2017). These enzymes are responsible for metabolizing GO and MGO, thus reducing the overall recovery rates in the transport experiment.

Proteins peptides and amino acids are widely present throughout the digestive system, and their presence can lead to the formation of multiple bound AGEs such as peptide-bound AGEs (Henle, 2005). This implies that proteins and amino acids may also exhibit scavenging activity towards food-borne AGE precursors that have already entered the digestive tract, thereby potentially reducing the bioavailability of the dicarbonyl compounds. We studied the transport of AGE precursors using DMEM containing amino acids with and without serum containing proteins, and compared it to transport in HBSS. The results obtained demonstrate that in HBSS, the concentrations of GO and MGO remained relatively constant over a 2-h period, while in DMEM with or without serum, a substantial decrease was observed, especially marked in MGO (Fig. 4). This explains why the transport of MGO in DMEM with or without serum was not completely linear in time but stabilized at a later stage over the 2-h transport experiment. This can best be attributed to the fact that DMEM contains relative high levels of amino acids, such as arginine hydrochloride (84 mg/L in DMEM) and lysine hydrochloride (146 mg/L in DMEM), which can react with GO and MGO, leading to the formation of AGEs (Treibmann, Venema and Henle, 2024). Furthermore, the presence of serum further increased the scavenging of the dicarbonyl precursors, likely due to the proteins present in serum (Nowotny, Jung, Höhn, Weber and Grune, 2015). In spite of this substantial scavenging, the transport of GO and MGO was not completely prevented. This suggests that the possible reactions of the dicarbonyl compounds with food constituents may reduce but will not fully eliminate their transport across the intestinal cells. We confirmed the formation of free MG-H1 by MGO in DMEM (with or without serum) (**Fig. S1**). Formation of CEL was not observed to a detectable level. MG-H1 is known to result from the interaction of MGO with arginine, while CEL would have been the result of a reaction of MGO with lysine, amino acids both present in DMEM. This preferred formation of MG-H1 over CEL is in line with results obtained in a recent study on the glycation reaction of dietary MGO and amines during digestion in the stomach and intestine using the TIM-1 model, confirming the generation of especially MG-H1 during digestion (Treibmann, Venema and Henle, 2024). Differences between the amount of the AGEs generated in our incubations and the TIM-1 model may be due to the fact that in the present study we only quantified free AGEs and did not also quantify bound forms, and to differences in the incubation conditions or duration.

It is of interest to note that GO and MGO can also be produced endogenously in intestinal cells and be maintained in a state of homeostasis (Twarda-Clapa, Olczak, Bialkowska and Koziolkiewicz, 2022). If GO and MGO from food accumulate in intestinal cells during absorption, the contribution of this external source compared to the endogenous levels will be decisive in whether the external exposure adds to the potential adverse consequences such as intracellular dicarbonyl or oxidative stress, protein damage and inflammatory responses. In our study, we observed that both GO and MGO accumulated in the intestinal cells but the intracellular accumulation is low at all concentration (Table 1). For CML at the same exposure concentration (125 μmol/L), the intracellular accumulation is 6.4- and 7.3- fold higher compared to that of GO and MGO. This strong intracellular retention of CML has also been reported in other studies (Tessier, Boulanger and Howsam, 2021), with some of the absorbed CML entering the circulation and some being retained in the enterocytes, resulting in a significant accumulation of free CML in the colon and ileum due to its hydrophilic nature, which makes it difficult to diffuse through the basolateral membrane (Hellwig et al., 2011; Yuan et al., 2022). Furthermore, the intracellular detoxification *via* a reaction with GSH and further conversion by the glyoxalase may be a factor contributing to the limited cellular accumulation of GO and MGO (Zheng, van Dongen, Bakker, Miro Estruch, & Rietjens, 2022).

Previous reports have confirmed the widespread presence of GO and MGO in everyday dietary sources such as alcoholic beverages, bread, coffee, and particularly in manuka honey, which is known to contain high levels of MGO (Majtan, 2011). The limited available *in vivo* studies have provided insights into the potential rapid degradation of MGO and the absence of MGO and its metabolites in urine (Degen, Vogel, Richter, Hellwig and Henle, 2013). However, the potential risk of adverse reactions resulting from GO and MGO entering the cells of the gastrointestinal tract remains unknown. With the present study, we confirmed that GO and MGO can be absorbed by the intestinal cells and translocated across the intestinal layer but how much the bioavailable fraction from food contributes to the total exposome, and whether this contribution is higher in intestinal cells than in other tissues has to await further studies.

Previous *in vivo* studies of CML, which was shown in the present study to pass the Caco-2 cellular membrane to a level comparable to that observed for GO and MGO, have reported that oral free CML can be detected in the blood of mice (Yuan et al., 2022) and rats (Yuan et al., 2023) and to accumulate in the kidneys and jejunum to a much higher extent than in other tissues. In the study reported by Alamir et al. (2013), CML was maintained in the circulation at no >1.5% of the total dose and this level returned to baseline after approximately 12 h. Based on the comparison to CML, the results of the present study indicate that the intestinal uptake of GO and MGO would be expected to be at least similar to that of CML, although their clearance within the intestinal cells or in the systemic circulation and tissues may be higher given their high reactivity and efficient scavenging by GSH and the glyoxalase system. This rapid clearance is supported by the absence of any GO or MGO or derived metabolites in urine, while for CML there was a positive correlation between oral intake and urinary excretion (Yuan et al., 2023).

5. Conclusion

To conclude, our study revealed that both GO and MGO can pass the intestinal layer through passive transport at least to an amount comparable to CML. Meanwhile, active transport remains, especially for GO. The reduced recovery of GO and MGO after 2 h transport experiment resulting from especially a decrease in the concentration at the apical side, and the reduced concentrations and transport rates in medium containing amino acids and protein as compared to HBSS point at their scavenging by food constituents, limiting but not fully preventing their bioavailability. Further research is needed to investigate the reactivity of GO and MGO in different food matrices and their stability and/or detoxification in the intestinal lumen. This study suggests that reactive

dicarbonyl AGE precursors from food will be bioavailable at least to some extent, thereby contributing to the overall endogenous exposome, although their relative contribution compared to endogenously formed AGE precursors remains to be established.

CRediT authorship contribution statement

Xiyu Li: Writing – original draft, Investigation, Data curation, Conceptualization. **Wouter Bakker:** Writing – review & editing, Methodology. **Yaxin Sang:** Writing – review & editing, Supervision. **Ivonne M.C.M. Rietjens:** Writing – review & editing, Supervision, Funding acquisition.

Declaration of competing interest

The authors declare no competing financial interest.

Data availability

Data will be made available on request.

Acknowledgment

The first author is supported by the China Scholarship Council (CSC) (grant number 202010230002), which is sincerely appreciated. Furthermore, we would like to acknowledge the reviewers of this paper, whose suggestions greatly improved it.

Appendix A. Supplementary data

Supplementary data to this article can be found online at https://doi.org/10.1016/j.foodchem.2024.139532.

References

Alamir, I., Niquet-Leridon, C., Jacolot, P., Rodriguez, C., Orosco, M., Anton, P. M., & Tessier, F. J. (2013). Digestibility of extruded proteins and metabolic transit of Nε-carboxymethyllysine in rats. *Amino Acids, 44*(6), 1441–1449. https://doi.org/10.1007/s00726-012-1427-3

Awortwe, C., Fasinu, P. S., & Rosenkranz, B. (2014). Application of Caco-2 cell line in herb-drug interaction studies: Current approaches and challenges. *Journal of Pharmaceutical Sciences, 17*(1), 1–19. https://doi.org/10.18433/j30k63

Bermudez-Brito, M., Munoz-Quezada, S., Gomez-Llorente, C., Matencio, E., Romero, F., & Gil, A. (2015). Lactobacillus paracasei CNCM I-4034 and its culture supernatant modulate Salmonella-induced inflammation in a novel transwell co-culture of human intestinal-like dendritic and Caco-2 cells. *BMC Microbiology, 15*(1). https://doi.org/10.1186/s12866-015-0408-6, 79, Article 79.

Cepas, V., Manig, F., Mayo, J. C., Hellwig, M., Collotta, D., Sanmartino, V., … Sainz, R. M. (2021). In Vitro Evaluation of the Toxicological Profile and Oxidative Stress of Relevant Diet-Related Advanced Glycation End Products and Related 1,2-Dicarbonyls. *Oxidative Medicine and Cellular Longevity, 2021*, 9912240. https://doi.org/10.1155/2021/9912240. Article 9912240.

Cha, J., Debnath, T., & Lee, K. G. (2019). Analysis of alpha-dicarbonyl compounds and volatiles formed in Maillard reaction model systems. *Scientific Reports, 9*(1), 5325. https://doi.org/10.1038/s41598-019-41824-8. Article 5325.

Degen, J., Vogel, M., Richter, D., Hellwig, M., & Henle, T. (2013). Metabolic transit of dietary methylglyoxal. *Journal of Agricultural and Food Chemistry, 61*(43), 10253–10260. https://doi.org/10.1021/jf304946p

Delgado-Andrade, C., & Fogliano, V. (2018). Dietary advanced glycosylation end-products (dAGEs) and Melanoidins formed through the Maillard reaction: Physiological consequences of their intake. *Annual Review of Food Science and Technology, 9*(1), 271–291. https://doi.org/10.1146/annurev-food-030117-012441

Delgado-Andrade, C., Tessier, F. J., Niquet-Leridon, C., Seiquer, I., & Pilar Navarro, M. (2012). Study of the urinary and faecal excretion of Nepsilon-carboxymethyllysine in young human volunteers. *Amino Acids, 43*(2), 595–602. https://doi.org/10.1007/s00726-011-1107-8

Ding, X., Hu, X., Chen, Y., Xie, J., Ying, M., Wang, Y., & Yu, Q. (2021). Differentiated Caco-2 cell models in food-intestine interaction study: Current applications and future trends. *Trends in Food Science & Technology, 107*, 455–465. https://doi.org/10.1016/j.tifs.2020.11.015

Förster, A., Kühne, Y., & Henle, T. (2005). Studies on absorption and elimination of dietary Maillard reaction products. *Annals of the New York Academy of Sciences*. https://doi.org/10.1196/annals.1333.054

Grunwald, S., Krause, R., Bruch, M., Henle, T., & Brandsch, M. (2006). Transepithelial flux of early and advanced glycation compounds across Caco-2 cell monolayers and their interaction with intestinal amino acid and peptide transport systems. *British Journal of Nutrition, 95*(6), 1221–1228. https://doi.org/10.1079/bjn20061793

Hellwig, M., Geissler, S., Matthes, R., Peto, A., Silow, C., Brandsch, M., & Henle, T. (2011). Transport of free and peptide-bound glycated amino acids: Synthesis, transepithelial flux at Caco-2 cell monolayers, and interaction with apical membrane transport proteins. *ChemBioChem, 12*(8), 1270–1279. https://doi.org/10.1002/cbic.201000759

Hellwig, M., Geissler, S., Peto, A., Knutter, I., Brandsch, M., & Henle, T. (2009). Transport of free and peptide-bound pyrraline at intestinal and renal epithelial cells. *Journal of Agricultural and Food Chemistry, 57*(14), 6474–6480. https://doi.org/10.1021/jf901224p

Hellwig, M., Gensberger-Reigl, S., Henle, T., & Pischetsrieder, M. (2018). Food-derived 1,2-dicarbonyl compounds and their role in diseases. *Seminars in Cancer Biology, 49*, 1–8. https://doi.org/10.1016/j.semcancer.2017.11.014

Hellwig, M., Matthes, R., Peto, A., Löbner, J., & Henle, T. (2014). N-ε-fructosyllysine and N-ε-carboxymethyllysine, but not lysinoalanine, are available for absorption after simulated gastrointestinal digestion. *Amino Acids, 46*(2), 289–299. https://doi.org/10.1007/s00726-013-1501-5

Henle, T. (2005). Protein-bound advanced glycation endproducts (AGEs) as bioactive amino acid derivatives in foods. *Amino Acids, 29*(4), 313–322. https://doi.org/10.1007/s00726-005-0200-2

Majtan, J. (2011). Methylglyoxal-a potential risk factor of Manuka honey in healing of diabetic ulcers. *Evidence-based Complementary and Alternative Medicine, 2011*, 1–5. https://doi.org/10.1093/ecam/neq013

Natoli, M., Leoni, B. D., D'Agnano, I., Zucco, F., & Felsani, A. (2012). Good Caco-2 cell culture practices. *Toxicology In Vitro, 26*(8), 1243–1246. https://doi.org/10.1016/j.tiv.2012.03.009

Nowotny, K., Jung, T., Höhn, A., Weber, D., & Grune, T. (2015). Advanced glycation end products and oxidative stress in type 2 diabetes mellitus. *Biomolecules, 5*(1), 194–222. https://doi.org/10.3390/biom5010194

Ravichandran, G., Lakshmanan, D. K., Raju, K., Elangovan, A., Nambirajan, G., Devanesan, A. A., & Thilagar, S. (2019). Food advanced glycation end products as potential endocrine disruptors: An emerging threat to contemporary and future generation. *Environment International, 123*, 486–500. https://doi.org/10.1016/j.envint.2018.12.032

Rietjens, I., Michael, A., Bolt, H. M., Simeon, B., Andrea, H., Nils, H., … Gerhard, E. (2022). The role of endogenous versus exogenous sources in the exposome of putative genotoxins and consequences for risk assessment. *Archives of Toxicology, 96*(5), 1297–1352. https://doi.org/10.1007/s00204-022-03242-0

Somoza, V., Wenzel, E., Weiss, C., Clawin-Radecker, I., Grubel, N., & Erbersdobler, H. F. (2006). Dose-dependent utilisation of casein-linked lysinoalanine, N(epsilon)-fructoselysine and N(epsilon)-carboxymethyllysine in rats. *Molecular Nutrition & Food Research, 50*(9), 833–841. https://doi.org/10.1002/mnfr.200600021

Tessier, F. J., Boulanger, E., & Howsam, M. (2021). Metabolic transit of dietary advanced glycation end-products - the case of N(E)-carboxymethyllysine. *Glycoconjugate Journal, 38*(3), 311–317. https://doi.org/10.1007/s10719-020-09950-y

Tessier, F. J., Niquet-Leridon, C., Jacolot, P., Jouquand, C., Genin, M., Schmidt, A. M., … Boulanger, E. (2016). Quantitative assessment of organ distribution of dietary protein-bound (13) C-labeled N(varepsilon) -carboxymethyllysine after a chronic oral exposure in mice. *Molecular Nutrition & Food Research, 60*(11), 2446–2456. https://doi.org/10.1002/mnfr.201600140

Treibmann, S., Groß, J., Pätzold, S., & Henle, T. (2022). Studies on the reaction of dietary methylglyoxal and Creatine during simulated gastrointestinal digestion and in human volunteers. *Nutrients, 14*(17), 3598. https://doi.org/10.3390/nu14173598

Treibmann, S., Venema, K., & Henle, T. (2024). Glycation reactions of methylglyoxal during digestion in a dynamic, in vitro model of the upper gastrointestinal tract (TIM-1). *Food Science & Nutrition*. https://doi.org/10.1002/fsn3.4118. *n/a*(n/a).

Twarda-Clapa, A., Olczak, A., Bialkowska, A. M., & Koziolkiewicz, M. (2022). Advanced glycation end-products (AGEs): Formation, chemistry, classification, receptors, and diseases related to AGEs. *Cells, 11*(8). https://doi.org/10.3390/cells11081312

van Dongen, K. C. W., Kappetein, L., Miro Estruch, I., Belzer, C., Beekmann, K., & Rietjens, I. (2022). Differences in kinetics and dynamics of endogenous versus exogenous advanced glycation end products (AGEs) and their precursors. *Food and Chemical Toxicology, 164*, 112987. https://doi.org/10.1016/j.fct.2022.112987. Article 112987.

Wang, X. J., Ma, S. B., Liu, Z. F., Li, H., & Gao, W. Y. (2019). Elevated levels of alpha-dicarbonyl compounds in the plasma of type II diabetics and their relevance with diabetic nephropathy. *Journal of Chromatography B: Analytical Technologies in the Biomedical and Life Sciences, 1106-1107*, 19–25. https://doi.org/10.1016/j.jchromb.2018.12.027

Wetzels, S., Wouters, K., Schalkwijk, C. G., Vanmierlo, T., & Hendriks, J. J. (2017). Methylglyoxal-derived advanced glycation Endproducts in multiple sclerosis. *International Journal of Molecular Sciences, 18*(2). https://doi.org/10.3390/ijms18020421

Wu, Q., Chen, Y., Ouyang, Y., He, Y., Xiao, J., Zhang, L., & Feng, N. (2021). Effect of catechin on dietary AGEs absorption and cytotoxicity in Caco-2 cells. *Food Chemistry, 355*, 129574. https://doi.org/10.1016/j.foodchem.2021.129574. Article 129574.

Wu, Q., Li, S. Y., Yang, T., Xiao, J., Chu, Q. M., Li, T., … Sun, Z. D. (2015). Inhibitory effect of lotus seedpod oligomeric procyanidins on advanced glycation end product formation in a lactose-lysine model system. *Electronic Journal of Biotechnology, 18*(2), 68–76. https://doi.org/10.1016/j.ejbt.2014.10.005

Wu, Y., Zong, M., Zhang, Z., Wu, Y., Li, L., Zhang, X., Wu, H., & Li, B. (2022). Selective transportation and energy homeostasis regulation of dietary advanced glycation end-products in human intestinal Caco-2 cells. *Food Chemistry, 391*, Article 133284. https://doi.org/10.1016/j.foodchem.2022.133284

Xu, H. Z., Wang, Z. Q., Wang, Y., Hu, S. D., & Liu, N. F. (2013). Biodistribution and elimination study of Fluorine-18 labeled N-epsilon-Carboxymethyl-lysine following Intragastric and intravenous administration. *PLoS One, 8*(3), e57897. https://doi.org/10.1371/journal.pone.0057897. Article e57897.

Yee, S. (1997). In vitro permeability across Caco-2 cells (colonic) can predict in vivo (small intestinal) absorption in man–fact or myth. *Pharmaceutical Research, 14*(6), 763–766. https://doi.org/10.1023/a:1012102522787

Yuan, X., Bai, Y., Zhang, J., Zhai, R., Nie, C., Tu, A., Li, S., Chen, Z., Zhang, M., & Li, J. (2022). Comparison of tissue distribution of free and protein bound Nvarepsilon-carboxymethyllysine after long-term oral administration to mice. *Food Research International, 161*, Article 111787. https://doi.org/10.1016/j.foodres.2022.111787

Yuan, X., Nie, C., Liu, H., Ma, Q., Peng, B., Zhang, M., Chen, Z., & Li, J. (2021). Comparison of metabolic fate, target organs, and microbiota interactions of free and bound dietary advanced glycation end products. *Critical Reviews in Food Science and Nutrition, 63*(19), 3612–3633. https://doi.org/10.1080/10408398.2021.1991265

Yuan, X., Zhai, R., Bai, Y., Zheng, M., Xie, X., Chen, T., Huang, T., Chen, Z., & Li, J. (2023). Comparison of pharmacokinetics, biodistribution, and excretion of free and bound Nε-carboxymethyllysine in rats by HPLC–MS/MS. *Food Research International, 164*, Article 112395. https://doi.org/10.1016/j.foodres.2022.112395

Zheng, L., van Dongen, K. C. W., Bakker, W., Miro Estruch, I., & Rietjens, I. (2022). The influence of intracellular glutathione levels on the induction of Nrf2-mediated gene expression by alpha-Dicarbonyl precursors of advanced glycation end products. *Nutrients, 14*(7). https://doi.org/10.3390/nu14071364. Article 1364.

Zhou, Q., Cheng, K. W., Gong, J., Li, E. T. S., & Wang, M. (2019). Apigenin and its methylglyoxal-adduct inhibit advanced glycation end products-induced oxidative stress and inflammation in endothelial cells. *Biochemical Pharmacology, 166*, 231–241. https://doi.org/10.1016/j.bcp.2019.05.027